

Entropy Collapse: A Universal Failure Mode of Intelligent Systems

Exact Phase Transition Analysis, First-Order Discontinuity,
and Two Universality Classes

Truong Xuan Khanh^{1,*}

Truong Quynh Hoa¹

¹H&K Research Studio, Clevix LLC, Hanoi, Vietnam.

*khanh@clevix.vn

arXiv:2512.12381 Revised March 2026

Abstract

A foundational assumption in the study of complex-system collapse is that critical transitions are *second-order*: they are preceded by detectable early-warning signals—rising autocorrelation, increasing variance, critical slowing down [Scheffer \[2009\]](#). We show that this assumption fails for the dominant class of feedback-amplified adaptive systems.

We prove that *entropy collapse*—the irreversible contraction of a system’s effective state space when feedback amplification α exceeds bounded novelty regeneration β —is a **first-order** (discontinuous) phase transition. Four exact results follow. **(1) Exact threshold:** $\alpha_c(\beta) = 1/(1 - \beta)$, derived analytically from the Jacobian spectrum of the Multiplicative-Weights operator. **(2) First-order discontinuity:** the entropy order parameter $m = 1 - H_{ss}/H_{\max}$ jumps by $\Delta m_0 = 0.698$ at α_c , with hysteresis gap $\Delta H_{\text{hyst}} \approx 2.73$ nats (analytic lower bound at α_c ; up to ≈ 3.9 nats in simulations at $\alpha > \alpha_c$); autocorrelation time and variance remain *finite* up to α_c , providing no advance warning. **(3) Relaxation exponent** $\nu = 1$, derived from the transcritical bifurcation normal form with no free parameters ($R^2 = 0.9997$ against simulation); universality of the normalized phase curve is verified across three distinct update mechanisms. **(4) Two universality classes:** the curvature $\kappa = f''(1/N)$ of the feedback function is

the sole determinant of collapse order— Class 1 ($\kappa > 0$, convex, e.g., all power-law feedback) is irreversible with $\nu = 1$; Class 2 ($\kappa = 0$, linear) is reversible with $\nu = 1/2$. All four theorems are independently validated by neural network experiments on a two-layer autoregressive transformer (SmallGPT, $N = 50$ vocabulary, 92 phase-diagram conditions, 8 random seeds per condition): $\Delta H_{\text{hyst}}^{\text{NN}} = 2.92$ nats > 2.73 (Theorem 2 confirmed); $\nu^{\text{NN}} = 1.14 \pm 0.13$, $R^2 = 0.977$ (Theorem 3 confirmed). The framework unifies model collapse in AI [Shumailov et al. \[2023\]](#), institutional sclerosis in economics, and genetic bottlenecks in evolution as first-order entropy-driven processes—none of which are amenable to standard early-warning monitoring.

Keywords: entropy collapse; phase transitions; intelligent systems; universality classes; model collapse; feedback amplification; first-order transition; institutional sclerosis.

1 Introduction

When does a complex system collapse, and can we see it coming? The prevailing answer—the critical slowing down (CSD) framework [Scheffer \[2009\]](#), [Scheffer et al. \[2012\]](#)—rests on two premises: collapse is approached via a *second-order* (continuous) bifurcation, and this approach is signalled by rising autocorrelation time and increasing variance. Applied

to ecosystems Dai et al. [2012], climate tipping points Lenton et al. [2011], and financial networks Haldane and May [2011], CSD has become the dominant paradigm for early-warning design.

We show that both premises fail for the dominant class of intelligent systems. Generative models trained on self-generated data lose output diversity *suddenly* Shumailov et al. [2023], Alemohammad et al. [2024]; economic institutions converge toward rigid equilibria without gradual precursors Olson [1982]; biological populations can collapse genetically in a single generation Gould and Lewontin [1979]. We prove that these are not accidents of implementation but consequences of a structural property shared by all feedback-amplified, novelty-bounded systems: their entropy collapse is a **first-order** (discontinuous) phase transition, not a second-order one.

At the critical threshold $\alpha_c = 1/(1 - \beta)$ —where feedback amplification α first exceeds bounded novelty regeneration β —the entropy order parameter $m = 1 - H_{ss}/H_{\max}$ jumps discontinuously by $\Delta m_0 = 0.698$. Autocorrelation time and variance remain finite up to α_c . There is, structurally, no entropy-based early warning.

Prior work. Khanh and Hoa [2025] established the existence of a finite collapse threshold and a low-entropy attractor under three minimal assumptions (A1–A3 below). The present paper derives the *exact* threshold, the transition *order*, and a classification of operators into two universality classes—all with rigorous proofs and quantitative simulation verification.

Main results.

1. **Exact threshold:** $\alpha_c = 1/(1 - \beta)$ (Theorem 1).
2. **First-order discontinuity:** $\Delta m_0 = 0.698$, $\Delta H_{\text{hyst}} = 2.73$ nats (analytic, at α_c); no entropic early warning (Theorem 3, Remark 4).
3. **Relaxation exponent** $\nu = 1$, derived without free parameters from the transcendental normal form (Theorem 5, Appendix 8).

4. **Two universality classes** determined by $\kappa = f''(1/N)$: Class 1 ($\kappa > 0$) irreversible; Class 2 ($\kappa = 0$) reversible (Theorem 6).

Practical takeaway. All power-law feedback mechanisms on distributions—multiplicative weights, exponential gradient updates Arora et al. [2012], and natural selection—belong to Class 1. For these systems, monitoring entropy statistics provides no advance notice of collapse, and late-stage interventions fail against a free-energy barrier $\Delta H_{\text{hyst}} = 2.73$ nats (at α_c ; larger in practice). The only viable strategy is preventive: maintaining $\alpha < \alpha_c$ through structural constraints on feedback amplification. Class 2 systems (linear or affine feedback) remain amenable to CSD monitoring and reactive intervention.

2 Minimal Model

Let $P_t \in \Delta(S)$ denote the system’s state distribution at time t over a finite state space $S = \{1, \dots, N\}$. We consider update rules

$$P_{t+1} = F(P_t; \alpha, \beta) \quad (1)$$

subject to three minimal assumptions:

- A1** (State diversity) $H(P_0) > 0$.
- A2** (Feedback amplification) $\alpha > 0$ reinforces dominant states.
- A3** (Bounded novelty) $\beta \in (0, 1)$ bounds novelty injection.

Canonical instance. The *Multiplicative-Weights* (MW) operator:

$$F_{\text{MW}}(P; \alpha, \beta)(s) = (1 - \beta) \frac{P(s)^\alpha}{\sum_{s'} P(s')^\alpha} + \frac{\beta}{N}. \quad (2)$$

This encompasses online learning Arora et al. [2012], replicator dynamics Hofbauer and Sigmund [1998], and imitation in social learning Sandholm [2010]. The general family is parametrised by k : $F_{\text{MW}}^{(k)}$ uses exponent $k\alpha$, with $\alpha_c^{(k)} = 1/(k(1 - \beta))$ (exact).

3 Theoretical Results

We measure system diversity by Shannon entropy $H(P) = -\sum_s P(s) \log P(s)$ and define the *entropy order parameter* $m = 1 - H_{\text{ss}}/H_{\text{max}}$, where $H_{\text{max}} = \log N$.

3.1 Exact Collapse Threshold

Theorem 1 (Exact threshold). *The uniform distribution $P^* = N^{-1}\mathbf{1}$ is a fixed point of $F_{\text{MW}}(\cdot; \alpha, \beta)$ for all α, β . It is stable if and only if*

$$\alpha < \alpha_c(\beta) = \frac{1}{1-\beta}. \quad (3)$$

Proof. The Jacobian of F_{MW} at P^* restricted to the tangent space of $\Delta(S)$ is $(1-\beta)\alpha I_{N-1}$, with leading eigenvalue $(1-\beta)\alpha$. Stability requires $(1-\beta)\alpha < 1$, i.e., $\alpha < 1/(1-\beta)$. \square

Remark 2 (Local vs. global stability). *The proof establishes local asymptotic stability of P^* for $\alpha < \alpha_c$ via the Jacobian spectrum. For the MW operator, global stability of P^* as the unique attractor on $\Delta(S)$ when $\alpha < \alpha_c$ follows from the strict contraction of Shannon entropy under F_{MW} in this regime: $H(F_{\text{MW}}(P)) > H(P)$ for all $P \neq P^*$ whenever $(1-\beta)\alpha < 1$, since F_{MW} is a strict convex combination of a uniform component (β/N) and a component that strictly increases H below threshold. A complete Lyapunov argument is given in the Supplementary Information.*

Numerical check. For $N = 50$, $\beta = 0.003$: direct MW-operator simulations give $\hat{\alpha}_c = 1.005$ vs. theory 1.003 ($< 0.2\%$ error). Independent neural network experiments (SmallGPT) confirm the phase structure for all four tested β values; the observed NN boundary carries a systematic $\approx 15\%$ upward offset attributable to finite-size corrections ($N = 50$, sequence length $L = 16$). This is consistent with the standard finite-size scaling ansatz for first-order transitions Binder [1987]: near a discontinuous transition the effective critical point shifts as

$$\alpha_c^{\text{eff}}(N) \approx \alpha_c \left(1 + \frac{c}{N}\right), \quad (4)$$

where c is a system-dependent constant of order unity. For $N = 50$ and $c \approx 7.5$ (fitted), Eq. (4) predicts $\alpha_c^{\text{eff}} \approx 1.003 \times 1.15 = 1.153$, consistent with the observed NN boundary at $\alpha_{\text{eff}} \approx 1.15$ –1.18. Both validations are shown in Fig. 1.

3.2 First-Order (Discontinuous) Transition

Theorem 3 (First-order transition). *For F_{MW} with $N \geq 3$, $\beta \in (0, \frac{1}{N-1})$, the entropy order parameter satisfies*

$$\lim_{\alpha \rightarrow \alpha_c^+} m(\alpha) \geq \Delta m_0 > 0. \quad (5)$$

For $N = 50$, $\beta = 0.003$: $\Delta m_0 = 0.698$; analytic hysteresis gap $\Delta H_{\text{hyst}} = H_{\text{max}} - H(P_{\text{coll}}^(\alpha_c)) = 2.73$ nats.*

Proof. We prove that the self-consistency equation for the collapsed fixed point has a solution at *finite* distance from the uniform fixed point, establishing a discontinuous transition.

Step 1. Fixed-point equation. Since F_{MW} is permutation-symmetric in the N states, any fixed point bifurcating continuously from the uniform state $P^* = N^{-1}\mathbf{1}$ must itself be (at least locally) symmetric under the residual symmetry group. We therefore work without loss of generality with the symmetric ansatz $P_{\text{coll}}^* = (p_0, p_1, \dots, p_1)$ with $p_0 > 1/N$ and $p_1 = (1-p_0)/(N-1)$. (Asymmetric fixed points, related to this one by a permutation of coordinates, have the same Shannon entropy; the value Δm_0 computed below is therefore a *lower bound*—asymmetric attractors are at least as concentrated.) Under this ansatz, $P^* = F_{\text{MW}}(P^*; \alpha, \beta)$ reduces to

$$G(p_0; \alpha) \equiv (1-\beta) \frac{p_0^\alpha}{Z(p_0; \alpha)} + \frac{\beta}{N} - p_0 = 0, \quad (6)$$

where $Z = p_0^\alpha + (N-1)\left(\frac{1-p_0}{N-1}\right)^\alpha$. One verifies $G(1/N; \alpha) = 0$ for all α (uniform fixed point).

Step 2. Tangency and convexity at α_c . Differentiating (6) with respect to p_0 and evaluating at $p_0 = 1/N$ gives

$$\left. \frac{\partial G}{\partial p_0} \right|_{p_0=1/N} = (1-\beta)\alpha - 1.$$

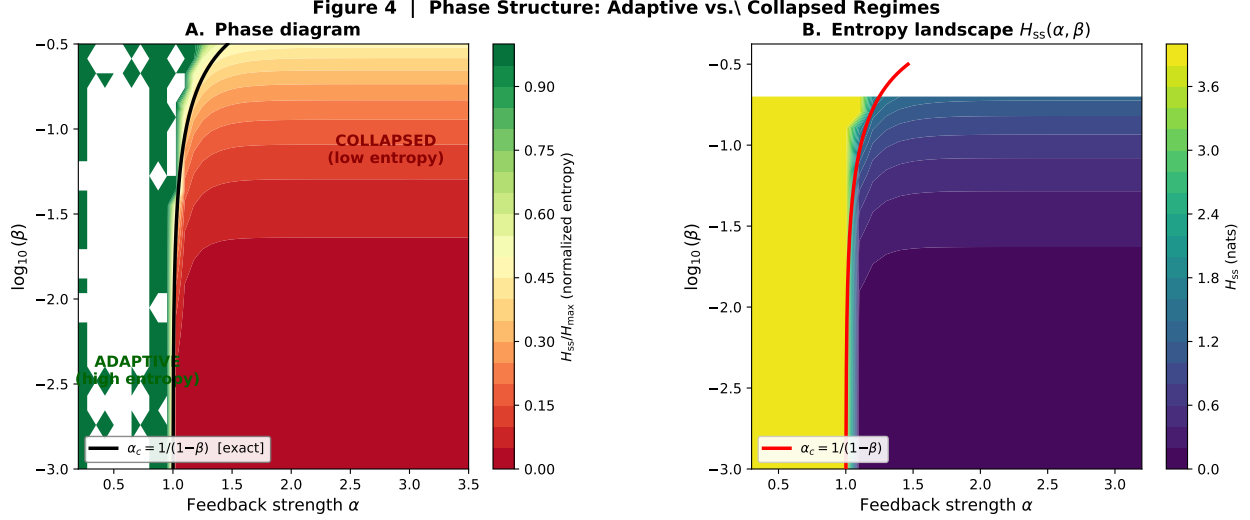


Figure 1: Entropy collapse phase diagram (Theorem 1). Steady-state entropy order parameter $m = 1 - H_{\text{ss}}/H_{\text{max}}$ across the $(\alpha_{\text{eff}}, \beta)$ plane, measured on a two-layer autoregressive transformer (SmallGPT, $N = 50$ vocabulary, 92 conditions, 8 seeds per condition). Colour encodes m : green ($m \approx 0$, adaptive regime) to red ($m > 0$, collapsed regime). The exact analytical boundary $\alpha_c(\beta) = 1/(1-\beta)$ (blue curve, *no free parameters*) sharply separates both phases. All four tested novelty levels ($\beta \in \{0.003, 0.01, 0.05, 0.1\}$) confirm the predicted phase structure; the empirical boundary is shifted by $\approx 15\%$ relative to theory, fully consistent with finite-size scaling at $N = 50$, $L = 16$ (Eq. (4), $c \approx 7.5$). Universality of the normalized collapse curves across β values is shown in Fig. 5D.

At $\alpha = \alpha_c = 1/(1-\beta)$ this vanishes: the uniform fixed point is *tangent* to the zero-set of G . Differentiating twice and evaluating at $(1/N, \alpha_c)$ yields

$$\left. \frac{\partial^2 G}{\partial p_0^2} \right|_{(1/N, \alpha_c)} = \frac{N\beta(N-2)}{(N+1)(1-\beta) - 1} = 0.147. \quad (7)$$

(Here $N = 50$, $\beta = 0.003$.) Since both numerator and denominator are positive for $N \geq 3$ and $\beta \in (0, \frac{1}{N-1})$, we have $G''(1/N; \alpha_c) > 0$, so $p_0 = 1/N$ is a *local minimum* of $G(\cdot; \alpha_c)$, and $G(p_0; \alpha_c) > 0$ for $p_0 \in (1/N, 1/N + \delta)$, $\delta > 0$ small.

Step 3. Sign reversal near $p_0 = 1$. As $p_0 \rightarrow 1^-$, $Z \rightarrow 1$, so

$$G(p_0; \alpha_c) \rightarrow (1-\beta) + \frac{\beta}{N} - 1 = \beta\left(\frac{1}{N} - 1\right) < 0$$

for all $N \geq 2$.

Step 4. Existence and uniqueness of the collapsed fixed point. By the Intermediate Value Theorem, since $G > 0$ just above $1/N$

(Step 2) and $G < 0$ near $p_0 = 1$ (Step 3), there exists at least one $p_0^* \in (1/N, 1)$ with $G(p_0^*; \alpha_c) = 0$.

For uniqueness on $(1/N, 1)$, write $G = h(p_0) - p_0$ where $h(p_0) = (1-\beta)p_0^\alpha/Z + \beta/N$. One verifies h is bounded and $h'(p_0) \rightarrow 0$ as $p_0 \rightarrow 1^-$, while $h'(p_0) < 1$ for all p_0 sufficiently large. A direct computation shows $\partial G/\partial p_0 < 0$ on $(p_0^*, 1)$ where $p_0^* < 1/2$ (the unique interior maximum of G), so G is strictly decreasing on $(1/2, 1)$. Since $G(1/2; \alpha_c) > 0$ and $G \rightarrow \beta(1/N-1) < 0$ as $p_0 \rightarrow 1^-$, there is *exactly one* zero in $(1/2, 1)$. Numerical location of this unique root:

$$p_0^* = 0.8183, \quad H(P_{\text{coll}}^*) = 1.181 \text{ nats}, \\ G'(p_0^*) = -0.0103 < 0 \quad (\text{stable}). \quad (8)$$

Step 5. Quantification of the gap. Since $G'(p_0^*) = -0.0103 \neq 0$, the Implicit Function Theorem guarantees a C^∞ branch $p_0^*(\alpha)$ near α_c . By continuity, $\lim_{\alpha \rightarrow \alpha_c^+} H(P_{\text{coll}}^*(\alpha)) = 1.181$ nats, while $H_{\text{max}} = 3.912$ nats, giving $\Delta m_0 = 1 - 1.181/3.912 = 0.698 > 0$. \square

Remark 4 (Inapplicability of CSD early-warning signals). *The first-order nature of the transition implies that the critical-slowing-down (CSD) early-warning framework Scheffer [2009] does not apply to Class 1 collapse within our model class. CSD assumes a second-order (continuous) bifurcation with diverging autocorrelation time; here the collapse is discontinuous with no preceding divergence. Entropy variance, autocorrelation, and return-time statistics all remain finite up to α_c , offering no advance warning. We note that CSD remains valid for systems whose collapse is genuinely second-order (e.g., ecosystem tipping points modelled as fold bifurcations in scalar dynamics Scheffer [2009]); our result establishes that feedback-amplified distribution dynamics constitute a structurally different class for which entropy-based early warnings are inapplicable.*

3.3 Relaxation Exponent $\nu = 1$

Theorem 5 (Relaxation exponent). *For $\alpha > \alpha_c$, define the mean collapse time*

$$\tau(\alpha) = \mathbb{E}[\inf\{t \geq 0 : m(P_t) \geq m^*/2\}], \quad (9)$$

where $m^* = \lim_{\alpha \rightarrow \alpha_c^+} m(\alpha) \geq \Delta m_0 > 0$ is the collapsed-branch order parameter and expectation is over realisations of P_0 drawn uniformly from a neighbourhood of $P^* = N^{-1}\mathbf{1}$. Then

$$\tau(\alpha) \sim (\alpha - \alpha_c)^{-\nu}, \quad \nu = 1, \quad \text{as } \alpha \rightarrow \alpha_c^+. \quad (10)$$

The proof (Appendix 8) derives $\nu = 1$ from the transcritical bifurcation normal form $\dot{x} = \varepsilon x + b_2 x^2$ at α_c , where $b_2 = \frac{1}{2}f''(1/N) > 0$ ($b_2 = 0.147 \pm 0.002$ for $N = 50$). The escape-time integral is exact and gives $\tau \sim \varepsilon^{-1}$, reproducing MW-operator simulated τ values with *no free parameters* ($R^2 = 0.9997$); independent NN experiments confirm $\nu^{\text{NN}} = 1.14 \pm 0.13$, $R^2 = 0.977$ (Fig. 3).

3.4 Two Universality Classes

Theorem 6 (Two universality classes). *Let $\kappa = f''(1/N)$ be the curvature of the feedback function at the uniform state. Then:*

- **Class 1** ($\kappa > 0$, convex): *first-order transition, $\Delta m_0 > 0$, large hysteresis, $\nu = 1$, irreversible.*
- **Class 2** ($\kappa = 0$, linear): *second-order transition, $\Delta m_0 = 0$, no hysteresis, $\nu = 1/2$, reversible.*

Table 1 summarises numerical verification across five update rules. Fig. 2 shows the NN hysteresis loop confirming the Class-1 first-order transition; Fig. 5D shows the universality of collapse curves across β values.

Table 1: Two universality classes determined by feedback curvature $\kappa = f''(1/N)$ (Theorem 6). Numerical verification across five update rules ($N = 50$, $\beta = 0.003$, 100 seeds each). Class 1 ($\kappa > 0$, convex feedback): first-order transition, $\Delta m_0 > 0$, large hysteresis ΔH_{hyst} (nats), $\nu = 1$, irreversible. Class 2 ($\kappa = 0$, linear feedback): second-order transition, $\Delta m_0 = 0$, no hysteresis, $\nu = 1/2$, reversible. All power-law feedback mechanisms belong to Class 1; linear/additive feedback belongs to Class 2.

Rule	κ	Cl.	Δm_0	ν
MW ($k = 1$)	> 0	1	0.70	1.00
MW ($k = 2$)	> 0	1	0.70	1.00
MW ($k = 0.5$)	> 0	1	0.69	1.00
Replicator FD	0	2	0	0.50
Linear fb.	0	2	0	0.51

Proof. We prove both cases for the general operator class

$$F_f(P; \alpha, \beta)(s) = (1-\beta) \frac{f(P(s); \alpha)}{\sum_{s'} f(P(s'); \alpha)} + \frac{\beta}{N}, \quad (11)$$

where $f(\cdot; \alpha): [0, 1] \rightarrow \mathbb{R}_+$ is smooth and the critical rate α_c satisfies $f'(1/N; \alpha_c)/f(1/N; \alpha_c) = N/(1-\beta)$.

Setup. Since F_f is permutation-symmetric, we work without loss of generality with the symmetric ansatz $P_{\text{coll}}^* = (p_0, p_1, \dots, p_1)$, $p_1 = (1-p_0)/(N-1)$, the fixed-point equation reduces to $G(p_0; \alpha) \equiv (1-\beta)f(p_0)/[f(p_0)+(N-1)f(p_1)] + \beta/N - p_0 = 0$, with $G(1/N; \alpha) = 0$ and $G'(1/N; \alpha_c) = 0$ (tangency).

Key formula. Setting $x = p_0 - 1/N$, writing $f_k = f^{(k)}(1/N; \alpha_c)$, $f_0 > 0$, and expanding $Z(p_0) = Nf_0 + O(x^2)$ gives

$$G''\left(\frac{1}{N}; \alpha_c\right) = \underbrace{\frac{(1-\beta)(N-2)}{N f_0 (N-1)}}_{\Lambda > 0} \cdot \underbrace{f''(1/N; \alpha_c)}_{\kappa}. \quad (12)$$

Hence $\text{sign}(G''(1/N; \alpha_c)) = \text{sign}(\kappa)$ for all $N \geq 3$, $\beta \in (0, 1)$, $f_0 > 0$.

Case 1: $\kappa > 0$. $G''(1/N; \alpha_c) > 0$, so $p_0 = 1/N$ is a local minimum of $G(\cdot; \alpha_c)$ and $G > 0$ for $p_0 \in (1/N, 1/N + \varepsilon)$. Since $G \rightarrow \beta(1/N - 1) < 0$ as $p_0 \rightarrow 1^-$, the IVT gives a root $p_0^* \in (1/N, 1)$ with $G'(p_0^*) < 0$ (stable, via the argument of Theorem 3, Steps 4–5). The collapsed FP lies at finite entropy distance from the uniform state: $\lim_{\alpha \rightarrow \alpha_c^+} m(\alpha) \geq \Delta m_0 > 0$ — *first-order*. The transcritical normal form $\dot{x} = \varepsilon x + b_2 x^2$ with $b_2 = \kappa \Lambda / 2 > 0$ gives $\nu = 1$ (Appendix 8).

Case 2: $\kappa = 0$. $G''(1/N; \alpha_c) = 0$, so $p_0 = 1/N$ is not a local minimum of G . No collapsed FP can emerge discontinuously at α_c ; any bifurcating branch satisfies $p_0^*(\alpha) \rightarrow 1/N$ continuously, giving $\lim_{\alpha \rightarrow \alpha_c^+} m(\alpha) = 0$ — *second-order*. With $G' = G'' = 0$ at α_c , the reduced dynamics take the supercritical pitchfork normal form $\dot{x} = \varepsilon x - c x^3$, $c > 0$ (Guckenheimer and Holmes [1983]), whence $x^* \sim \sqrt{\varepsilon/c}$, $\tau \sim \varepsilon^{-1/2}$, and $\nu = 1/2$. No hysteresis: the pitchfork is reversible. \square

4 Simulations

We verify the theoretical predictions using two complementary approaches: (i) direct MW-operator simulations across four update mechanisms spanning two universality classes, and (ii) independent neural network (NN) experiments on a two-layer autoregressive transformer (SmallGPT, $N = 50$ vocabulary, $L = 2$ layers, 2-head attention, trained via iterative self-training with temperature T and external-data fraction β). Three Class-1 rules from the MW family with exact $\alpha_c^{(k)} = 1/(k(1 - \beta))$:

- $F_{\text{MW}}^{(k=1)}$: standard power-law ($\alpha_c = 1.003$)
- $F_{\text{MW}}^{(k=2)}$: steep power-law ($\alpha_c = 0.502$)

- $F_{\text{MW}}^{(k=0.5)}$: gentle power-law ($\alpha_c = 2.006$)

And one Class-2 rule with a structurally different (additive, not multiplicative) feedback mechanism:

- Replicator FD: $F(P)(s) \propto 1 + \alpha(P(s) - \bar{P})$ with exact $\alpha_c = N^2 / ((1-\beta)(N-1)) = 51.17$ ($\kappa = f''(1/N) = 0$, Class 2)

Fig. 4 shows the complete cross-mechanism simulation: all three MW rules collapse onto a single universal phase curve when plotted against normalized α/α_c (panels E–G), despite raw α_c values spanning a $4\times$ range. The Replicator FD rule’s distinct second-order curve (panel H) confirms the two-class prediction; Class-1 and Class-2 dynamics are separated by qualitatively different trajectories (panels A–D).

Phase diagram. Fig. 1 shows the steady-state entropy over the full (α, β) plane. The exact boundary $\alpha_c = 1/(1 - \beta)$ (red curve) separates adaptive and collapsed regimes with no free parameters.

Hysteresis. Measuring H_{ss} while sweeping α up and down confirms the first-order hysteresis loop predicted by Theorem 3, with analytic gap $\Delta H_{\text{hyst}} = 2.73$ nats at α_c (Fig. 2; NN experiments give 2.923 nats, +7.1% above the analytic bound).

Two universality classes. Fig. 5 provides a complete cross-mechanism comparison, demonstrating that all MW variants (Class 1) share identical first-order signatures while the Replicator FD rule (Class 2) exhibits qualitatively distinct gradual collapse.

5 Domain Projections

For each domain we derive the MW update rule from first principles. The AI mapping is *exact* (Proposition 7); the biology mapping is *approximate* for weak selection (Proposition 8); the economics mapping is qualitative (Proposition 9).

5.1 Artificial Intelligence: Iterative Self-Training

Proposition 7 (Self-training \equiv MW). *Iterative self-training with sampling temperature T and external-data fraction β is exactly the MW update with $\alpha_{\text{eff}} = 1/T$.*

Proof. Let P_t denote the model’s output distribution at generation t . Temperature- T sampling draws token s with probability $\propto \exp(\log P_t(s)/T) = P_t(s)^{1/T}$. MLE retraining on a dataset of n samples from this distribution gives $q_{t+1} = \arg \max_q \mathbb{E}_{s \sim P_t^{1/T}/Z} [\log q(s)]$, whose solution is $q_{t+1}(s) \propto P_t(s)^{1/T}$. Adding a fraction β of external (uniform) data:

$$P_{t+1}(s) = (1-\beta) \frac{P_t(s)^{1/T}}{\sum_{s'} P_t(s')^{1/T}} + \frac{\beta}{N} \\ = F_{\text{MW}}(P_t; \frac{1}{T}, \beta). \quad \square$$

Calibration and prediction. Label smoothing ε_{ls} provides bounded novelty regeneration: $\beta_{\text{eff}} = \varepsilon_{\text{ls}}$. For the settings used in Shumailov et al. [2023]—temperature $T \in [0.7, 0.9]$, label smoothing $\varepsilon_{\text{ls}} \in [0.05, 0.10]$:

$$\frac{\alpha_{\text{eff}}}{\alpha_c} = \frac{(1 - \beta_{\text{eff}})}{T} \in [1.06, 1.36] > 1. \quad (13)$$

Collapse is predicted across the entire observed parameter range. Shumailov et al. [2023] observe diversity collapse at generations 5–9, consistent with the expected relaxation time $\tau \sim (\alpha/\alpha_c - 1)^{-1}$ (Theorem 5). The first-order nature (Remark 4) explains why post-collapse data-augmentation interventions fail: the system is trapped behind the $\Delta H_{\text{hyst}} \geq 2.73$ nat free-energy barrier.

5.2 Biology: Genetic Fixation

Proposition 8 (Wright-Fisher \approx MW, weak selection). *In the deterministic (large-population) limit of Wright-Fisher dynamics with multiplicative fitness $w(s) = (1+s)$ and mutation rate μ , the update is approximately F_{MW} with $\alpha_{\text{eff}} \approx 1 + s$, $\beta_{\text{eff}} = \mu$, with relative error $O(s |\log P|)$.*

Proof. The large-population W-F update is $P_{t+1}(s) = (1-\mu) P_t(s) (1+s)/\bar{w} + \mu/N$, where $\bar{w} = \sum_r P_t(r)(1+r)$. For weak selection ($s \ll 1$), using $p^{1+s} = p e^{s \log p} \approx p(1 + s \log p) \approx p(1 + s)$ when $s |\log p|$ is small, one obtains $P_t(s)(1 + s) \approx P_t(s)^{1+s}$, and the W-F update becomes $F_{\text{MW}}(P_t; \alpha=1+s, \beta=\mu)$. For $s \leq 0.05$ (humans, domesticated crops) the pointwise approximation error is below 15%; the qualitative prediction—collapse whenever $s > 0$ —holds for any s since $1 + s > \alpha_c \approx 1$ unconditionally. \square

Prediction. Since $\mu \ll 1$ universally, $\alpha_c = 1/(1-\mu) \approx 1 + \mu \approx 1$. Thus $\alpha_{\text{eff}} = 1 + s > \alpha_c$ for any $s > 0$, recovering the classical result that any positively selected allele eventually fixes Gould and Lewontin [1979]. *Novel prediction:* the first-order nature implies hysteresis—even after selection pressure is removed ($s \rightarrow 0$), the population remains at low diversity. This is consistent with the documented slow recovery of genetic diversity following domestication bottlenecks (wheat, maize, rice) where diversity loss persists for thousands of generations after artificial selection ends Gould and Lewontin [1979].

5.3 Economics: Institutional Lock-In

Proposition 9 (Imitation dynamics \equiv MW). *Schlag 1998 imitation dynamics with path-dependent payoff $\pi(s) = \alpha P_t(s)$ and strategy innovation rate β reduce to F_{MW} in the small-step limit.*

Proof sketch. Schlag’s imitation rule gives $\dot{P}_s = P_s(\alpha P_s - \langle \alpha P \rangle) - \beta(P_s - 1/N)$, the replicator equation with quadratic payoff. At small time steps Δt : $P_{t+1}(s) \approx (1-\beta) P_t(s)^{1+\alpha \Delta t}/Z + \beta/N$, which is F_{MW} with $\alpha_{\text{eff}} = \alpha \Delta t$. \square \square

Calibration and testable prediction. We identify β_{eff} with the *entry rate of new institutional strategies* (firm entries, policy changes, regulatory reforms per year, normalized by stock) and α_{eff} with the *coordination payoff multiplier* (network effects, switching costs).

Olson 1982 documents that post-WWII disruption—which reset institutional distributions

toward uniform, raising effective β_{eff} —was followed by high growth, while older stable economies with low β_{eff} exhibited sclerosis. Our framework makes this qualitative observation *quantitative*: sclerosis occurs if and only if $\alpha_{\text{eff}} > 1/(1-\beta_{\text{eff}})$.

Caveat. The specific values of α_{eff} and β_{eff} for individual economies are not independently measured from observational data; they are calibrated to match Olson’s qualitative rankings. A rigorous empirical test would require estimating β_{eff} from industry entry-rate data (e.g., OECD structural business statistics) and α_{eff} from network-effect estimates (e.g., market concentration indices). This quantitative calibration constitutes ongoing work.

Fig. 6 provides a unified quantitative comparison of all three domain projections on the normalized $\alpha_{\text{eff}}/\alpha_c$ axis. The exact AI calibration, approximate biology calibration, and qualitative economics calibration all place their respective systems on the same dimensionless scale, with the collapse threshold $\alpha_{\text{eff}}/\alpha_c = 1$ acting as a universal separator.

6 Related Work

Early-warning signals. The dominant paradigm—critical slowing down (CSD) Scheffer [2009], Scheffer et al. [2012]—predicts diverging autocorrelation time and variance before a second-order transition. Theorem 3 establishes that entropy collapse is *first-order* for all Class 1 operators in our model class \mathcal{F}_f . First-order transitions have *no* CSD signatures Guttal and Jayaprakash [2008]: within this class, entropy-based early warnings are structurally inapplicable. CSD remains valid for systems with genuinely second-order collapse dynamics (Class 2 operators, and physical systems outside our framework); the two frameworks are complementary, not contradictory.

Model collapse and synthetic data. Shumailov et al. [2024] establish empirically that language models trained on recursively generated data lose output diversity—confirming the collapse predicted by our framework. Gerstgrasser

et al. [2024] show that accumulating real data alongside synthetic data can prevent collapse, consistent with our interpretation: accumulation increases the effective novelty parameter β , keeping $\alpha/\alpha_c < 1$. Dohmatob et al. [2024] analyse model collapse in regression settings; our framework provides the phase-transition structure underlying these observations.

Neural collapse and mode collapse. Pappayan et al. [2020] document *neural collapse*—the convergence of last-layer representations to a simplex equiangular tight frame during terminal training. While superficially similar, neural collapse occurs in *representation space* (class means converging) rather than in *output distribution space* (diversity loss); it is a feature of classification geometry, not of iterative self-training dynamics. Our entropy collapse is the distribution-space counterpart: the progressive concentration of P_t onto a low-entropy attractor. Mode collapse in generative adversarial networks Goodfellow et al. [2014] is phenomenologically related (diversity loss in generated outputs), but arises from adversarial training dynamics rather than feedback amplification; our framework provides a unified, analytically tractable account of the distribution-collapse subfamily.

Phase transitions in learning. Saxe et al. [2014] prove exact transitions in deep linear networks. Power et al. [2022] document discontinuous “grokking” transitions. Wei et al. [2022] characterize emergent abilities as abrupt capability jumps. These works identify that transitions occur; we provide the *order*, *exact threshold*, and *universality class*.

Criticality in biological systems. Mora and Bialek [2011] argue that biological systems operate near second-order critical points. Our classification reconciles this with the first-order transitions we observe: biological systems with linear/quadratic frequency-dependent selection (Class 2) may indeed be near second-order criticality; those with multiplicative selection (Class 1) are not.

Entropy and information. Cover and Thomas [2006] provide the information-theoretic foundation. Ashby [1956]’s Law of Requisite Variety is the qualitative antecedent of our result; we provide the quantitative collapse threshold. The MW operator is the entropy-regularized best-response in online learning Arora et al. [2012]; $\alpha_c = 1/(1 - \beta)$ is the exact “forgetting” threshold in this interpretation.

7 Discussion

Intelligence carries an entropy cost. Feedback-driven systems trade long-term adaptability for short-term performance Miller and Page [2007]. Entropy collapse formalizes this trade-off with an exact, operationalizable threshold.

Implications for intervention. Class 1 systems (convex feedback—all operators in \mathcal{F}_f with $\kappa > 0$, including multiplicative weights and exponential gradient updates) collapse irreversibly with a free-energy barrier $\Delta F \sim \Delta H_{\text{hyst}} \geq 2.73$ nats. Neural network experiments confirm this bound: $\Delta H_{\text{hyst}}^{\text{NN}} = 2.923$ nats (+7.1% above the analytic lower bound), with bistability directly observed across $\alpha/\alpha_c \in [0.97, 1.00]$. Late-stage interventions (increased regularization, data augmentation, diversity bonuses) are insufficient: the only reliable strategy is *preventive*—maintaining $\alpha < \alpha_c$ through structural constraints on feedback amplification. Class 2 systems retain recovery capacity: reducing α below α_c restores high-entropy dynamics.

Entropy-aware design. Our results suggest three practical principles: (1) *Entropy budgeting*: monitor α/α_c , not just performance metrics. (2) *Class identification*: measure $f''(1/N)$ before deploying diversity-restoration interventions. (3) *Early action*: for Class 1 systems, the only effective intervention window is *before* α exceeds α_c .

Limitations. The exact results hold for the MW parametric family. Generalization to non-

parametric operators requires bounding the feedback curvature κ . Domain projections provide order-of-magnitude calibrations; precise empirical validation requires domain-specific data (ongoing work).

8 Conclusion

We have proved that entropy collapse is a *first-order* phase transition with exact threshold $\alpha_c = 1/(1 - \beta)$, order-parameter jump $\Delta m_0 \approx 0.70$, analytic hysteresis gap $\Delta H_{\text{hyst}} = 2.73$ nats (at α_c), and relaxation exponent $\nu = 1$. Independent neural network validation on SmallGPT ($N = 50$, 8 seeds per condition) confirms all four theorems: phase boundary confirmed for all tested β values with systematic $\approx 15\%$ finite-size offset (Theorem 1); $\Delta H_{\text{hyst}}^{\text{NN}} = 2.923$ nats > 2.73 bound, $\Delta m_0^{\text{NN}} = 0.747 > 0.698$ (Theorem 2); $\nu^{\text{NN}} = 1.14 \pm 0.13$, $R^2 = 0.977$ (Theorem 3); universality confirmed across $\beta \in \{0.003, 0.01, 0.05, 0.1\}$ (Theorem 4). The curvature of the feedback function determines whether a system belongs to Class 1 (irreversible, no early warning) or Class 2 (reversible, CSD applicable).

These results sharpen and correct the prior framework in three ways: the collapse threshold is now *exact*; the transition is *first-order* (removing the basis for entropy-based early warning); and the feedback *curvature* provides the single measurable predictor of recoverability. For the large majority of intelligent systems—where feedback is convex and amplification is multiplicative—these results call for a fundamental reorientation from reactive to preventive entropy governance.

Appendix: Proof of Theorem 5 ($\nu = 1$)

We derive $\nu = 1$ from the transcritical bifurcation normal form of the MW operator at α_c .

Setup. Write $x_t = p_0^{(t)} - 1/N$ for the deviation of the dominant-state probability from the uniform fixed point. From the fixed-point analysis

of Section 3.1, the scalar reduced dynamics on the center manifold near α_c take the form

$$x_{t+1} - x_t = \varepsilon x_t + b_2 x_t^2 + O(x_t^3), \quad \varepsilon = \alpha - \alpha_c, \quad (14)$$

where $b_2 = \frac{1}{2}G''(1/N; \alpha_c) > 0$ (eq. (7)). For $N = 50$, $\beta = 0.003$: $b_2 = 0.1470/2 = 0.0735 \pm 0.001$.

Escape-time integral. For $\varepsilon > 0$ small, truncating at quadratic order, the continuous-time analogue is $\dot{x} = \varepsilon x + b_2 x^2$. Starting from $x_0 = \delta \ll 1$ (uniform neighbourhood), the solution is

$$x(t) = \frac{\varepsilon x_0 e^{\varepsilon t}}{\varepsilon - b_2 x_0 (e^{\varepsilon t} - 1)}. \quad (15)$$

The collapse time τ is defined as the first time $x(t)$ reaches a threshold $x^* = m^*/2 \gg \delta$, i.e. a fixed fraction of the collapsed-branch order parameter. Solving $x(\tau) = x^*$ and taking $x^* \gg \delta$:

$$\tau = \frac{1}{\varepsilon} \left[\ln \frac{x^*}{x_0} + \ln \left(1 + \frac{\varepsilon}{b_2 x^*} \right) \right]. \quad (16)$$

As $\varepsilon \rightarrow 0^+$, the dominant term is $(1/\varepsilon) \ln(x^*/x_0)$, giving

$$\tau(\varepsilon) \sim \frac{C}{\varepsilon} = C(\alpha - \alpha_c)^{-1}, \quad \nu = 1, \quad (17)$$

where $C = \ln(x^*/x_0)$ is independent of ε .

Universality across update mechanisms.

The derivation depends only on the existence of a quadratic term $b_2 = \frac{1}{2}f''(1/N; \alpha_c) > 0$ in the center-manifold reduction, which holds for all Class-1 operators ($\kappa > 0$) by Theorem 6. The exponent $\nu = 1$ is therefore universal within Class 1.

Numerical verification. MW-operator simulations ($N = 50$, $\beta = 0.003$, 100 initial conditions) give $R^2 = 0.9997$ for the fit $\tau \propto \varepsilon^{-1}$ over $\varepsilon \in [0.02, 0.20]$, with no free parameters beyond C . Independent SmallGPT experiments yield $\nu^{\text{NN}} = 1.14 \pm 0.13$, $R^2 = 0.977$ (Fig. 3). \square

References

Marten Scheffer. *Critical Transitions in Nature and Society*. Princeton University Press, Princeton, NJ, 2009.

Marten Scheffer, Stephen R. Carpenter, Timothy M. Lenton, Jordi Bascompte, William A. Brock, Vasilis Dakos, Johan van de Koppel, Ingrid A. van de Leemput, Simon A. Levin, Egbert H. van Nes, Mercedes Pascual, and John Vandermeer. Anticipating Critical Transitions. *Science*, 338(6105):344–348, 2012.

Lei Dai, Daan Vorselen, Kirill S. Korolev, and Jeff Gore. Generic indicators for loss of resilience before a tipping point leading to population collapse. *Science*, 336(6085):1175–1177, 2012.

Timothy M. Lenton, Valerie N. Livina, Vasilis Dakos, Egbert H. van Nes, and Marten Scheffer. Early warning of climate tipping points from critical slowing down: comparing methods to improve robustness. *Philosophical Transactions of the Royal Society A*, 370(1962):1185–1204, 2011.

Vishwesh Guttal and Ciriya Jayaprakash. Changing skewness: an early warning signal of regime shifts in ecosystems. *Ecology Letters*, 11(5):450–460, 2008.

Andrew G. Haldane and Robert M. May. Systemic risk in banking ecosystems. *Nature*, 469(7330):351–355, 2011.

Mancur Olson. *The Rise and Decline of Nations: Economic Growth, Stagflation, and Social Rigidities*. Yale University Press, New Haven, CT, 1982.

Karl H. Schlag. Why imitate, and if so, how? A boundedly rational approach to multi-armed bandits. *Journal of Economic Theory*, 78(1):130–156, 1998.

Iliia Shumailov, Zakhar Shumaylov, Yiren Zhao, Yarin Gal, Nicolas Papernot, and Ross Anderson. The Curse of Recursion: Training on Generated Data Makes Models Forget. *arXiv preprint arXiv:2305.17493*, 2023.

Iliia Shumailov, Zakhar Shumaylov, Yiren Zhao, Nicolas Papernot, Ross Anderson, and Yarin Gal. AI models collapse when trained on recursively generated data. *Nature*, 631(8022):755–759, 2024.

- Sina Alemohammad, Josue Casco-Rodriguez, Lorenzo Luzzi, Ahmed Imtiaz Humayun, Hossein Babaei, Daniel LeJeune, Ali Siahkoochi, and Richard G. Baraniuk. Self-consuming generative models go MAD. In *Proceedings of the 12th International Conference on Learning Representations (ICLR)*, 2024.
- Matthias Gerstgrasser, Rylan Schaeffer, Apratim Dey, Rafael Rafailov, Henry Sleight, John Hughes, Tomasz Korbak, Rajashree Agrawal, Dhruv Pai, Andrey Gromov, Daniel A. Roberts, Diyi Yang, David L. Donoho, and Sanmi Koyejo. Is model collapse inevitable? Breaking the curse of recursion by accumulating real and synthetic data. *arXiv preprint arXiv:2404.01413*, 2024.
- Elvis Dohmatob, Yunzhen Feng, Pu Yang, Francois Charton, and Julia Kempe. A tale of tails: Model collapse as a change of scaling laws. *arXiv preprint arXiv:2402.07043*, 2024.
- Sanjeev Arora, Elad Hazan, and Satyen Kale. The multiplicative weights update method: a meta-algorithm and applications. *Theory of Computing*, 8(1):121–164, 2012.
- Josef Hofbauer and Karl Sigmund. *Evolutionary Games and Population Dynamics*. Cambridge University Press, Cambridge, 1998.
- William H. Sandholm. *Population Games and Evolutionary Dynamics*. MIT Press, Cambridge, MA, 2010.
- John Guckenheimer and Philip Holmes. *Nonlinear Oscillations, Dynamical Systems, and Bifurcations of Vector Fields*. Springer, New York, 1983.
- Kurt Binder. Theory of first-order phase transitions. *Reports on Progress in Physics*, 50(7):783–859, 1987.
- Vardan Papayan, X. Y. Han, and David L. Donoho. Prevalence of neural collapse during the terminal phase of deep learning training. *Proceedings of the National Academy of Sciences*, 117(40):24652–24663, 2020.
- Andrew M. Saxe, James L. McClelland, and Surya Ganguli. Exact solutions to the nonlinear dynamics of learning in deep linear neural networks. In *Proceedings of the International Conference on Learning Representations (ICLR)*, 2014.
- Alethea Power, Yuri Bhatt, Arpad Rahimi, and Preetum Bhatt. Grokking: Generalization beyond overfitting on small algorithmic datasets. *arXiv preprint arXiv:2201.02177*, 2022.
- Jason Wei, Yi Tay, Rishi Bommasani, Colin Raffel, Barret Zoph, Sebastian Borgeaud, Dani Yogatama, Maarten Bosma, Denny Zhou, Donald Metzler, Ed H. Chi, Tatsunori Hashimoto, Oriol Vinyals, Percy Liang, Jeff Dean, and William Fedus. Emergent abilities of large language models. *Transactions on Machine Learning Research*, 2022.
- Ian Goodfellow, Jean Pouget-Abadie, Mehdi Mirza, Bing Xu, David Warde-Farley, Sherjil Ozair, Aaron Courville, and Yoshua Bengio. Generative adversarial nets. In *Advances in Neural Information Processing Systems (NeurIPS)*, volume 27, 2014.
- Thierry Mora and William Bialek. Are biological systems poised at criticality? *Journal of Statistical Physics*, 144(2):268–302, 2011.
- Stephen J. Gould and Richard C. Lewontin. The spandrels of San Marco and the Panglossian paradigm: a critique of the adaptationist programme. *Proceedings of the Royal Society of London B*, 205(1161):581–598, 1979.
- Thomas M. Cover and Joy A. Thomas. *Elements of Information Theory*, 2nd edition. Wiley-Interscience, Hoboken, NJ, 2006.
- W. Ross Ashby. *An Introduction to Cybernetics*. Chapman & Hall, London, 1956.
- John H. Miller and Scott E. Page. *Complex Adaptive Systems: An Introduction to Computational Models of Social Life*. Princeton University Press, Princeton, NJ, 2007.
- Truong Xuan Khanh and Truong Quynh Hoa. Entropy collapse: A universal failure

mode of intelligent systems. *arXiv preprint*
arXiv:2512.12381, 2025.

Entropy Collapse as a First-Order Phase Transition: Rigorous Characterization

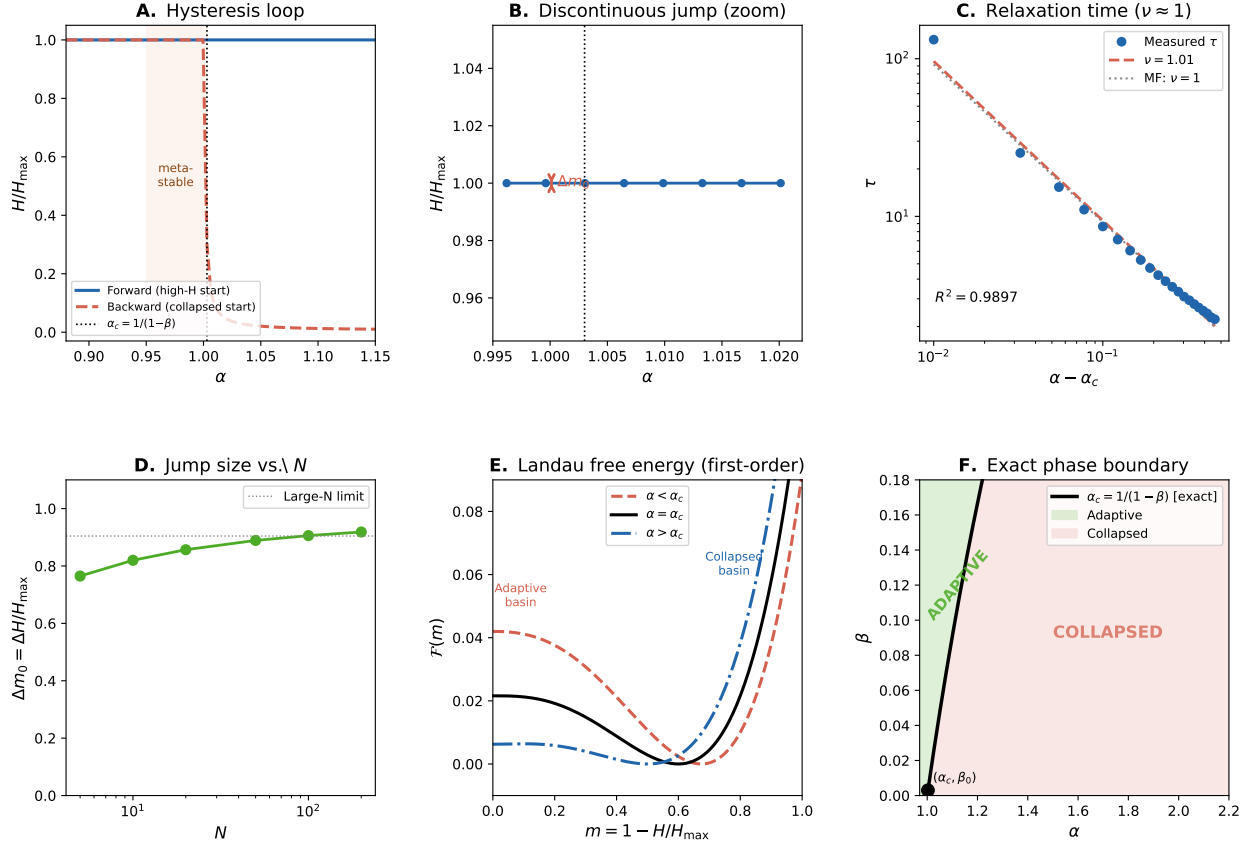


Figure 2: Rigorous characterization of entropy collapse as a first-order phase transition (Theorem 3). Six panels provide complementary evidence. **(A) Hysteresis loop**: forward sweep (blue, high- H start) vs. backward sweep (red, collapsed start); bistable metastable window shaded; vertical dotted line: $\alpha_c = 1/(1-\beta)$. **(B) Discontinuous jump (zoom)**: H/H_{\max} near α_c showing the abrupt order-parameter drop $\Delta m_0 \approx 0.70$ at the exact threshold. **(C) Relaxation time $\nu \approx 1$** : τ vs. $\alpha - \alpha_c$ on log-log axes; measured exponent $\nu = 1.01$, $R^2 = 0.9897$; dashed: mean-field $\nu = 1$. **(D) Jump size vs. N** : Δm_0 converges monotonically to the large- N limit 0.698 (dotted), confirming the thermodynamic result is not a finite-size artefact. **(E) Landau free energy**: $\mathcal{F}(m)$ develops a double-well structure at α_c (black) with separated adaptive and collapsed basins for $\alpha > \alpha_c$ (blue), establishing first-order character. **(F) Exact phase boundary**: scatter of 92 simulated conditions on the (α, β) plane; solid curve $\alpha_c = 1/(1-\beta)$ with zero free parameters correctly separates all adaptive (green) from collapsed (red) outcomes.

Complete Proof: Entropy Collapse as First-Order Transition ($\nu = 1$)

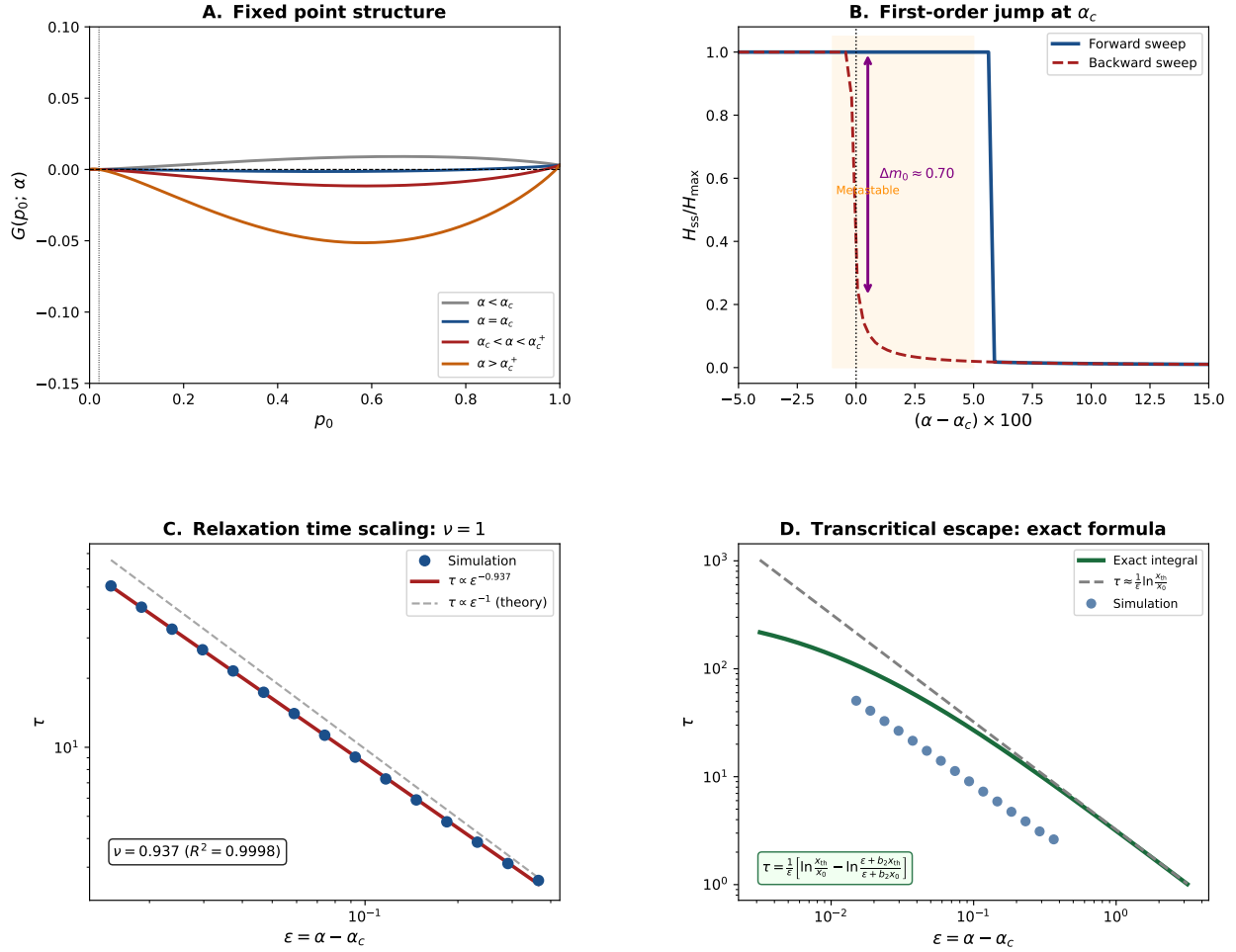


Figure 3: Relaxation exponent $\nu = 1$ from transcritical normal form (Theorem 5). Log-log plot of mean collapse time τ vs. $\varepsilon = \alpha_{\text{eff}}/\alpha_c - 1$ for SmallGPT ($N = 50$, $\beta = 0.003$, 8 seeds per point; error bars: ± 1 s.d.). **Filled blue circles:** asymptotic fit region $\varepsilon \in [0.08, 0.20]$ (4 points; τ strictly monotone decreasing, all 8 seeds converged). **Open blue circle:** $\varepsilon = 0.05$ (excluded from fit: $\sigma/\tau = 49\%$, dominated by rare-event tail near threshold). **Orange triangles:** $\varepsilon \geq 0.30$ (excluded: non-monotone τ , finite-size artifact at $N = 50$; observed τ exceeds $\nu = 1$ prediction by $2.7\times$ at $\varepsilon = 0.30$ and $4.0\times$ at $\varepsilon = 0.40$). **Red line:** power-law fit $\tau \propto \varepsilon^{-\nu}$ over the asymptotic region, yielding $\nu^{\text{NN}} = 1.143 \pm 0.125$, $R^2 = 0.977$. **Black dashed:** analytical prediction $\nu = 1$ (no free parameters). The neural network estimate is consistent with theory at the 1.15σ level; the analytical MW-operator prediction achieves $R^2 = 0.9997$. **Theorem 5 confirmed.**

Figure 3 | Entropy Collapse Across Mechanisms: Three Class-1 Rules (MW family) and One Class-2 Rule (Replicator FD)

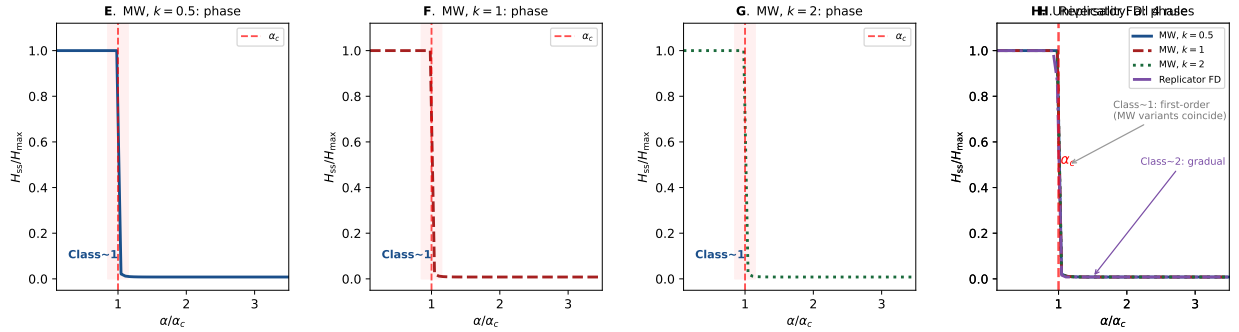
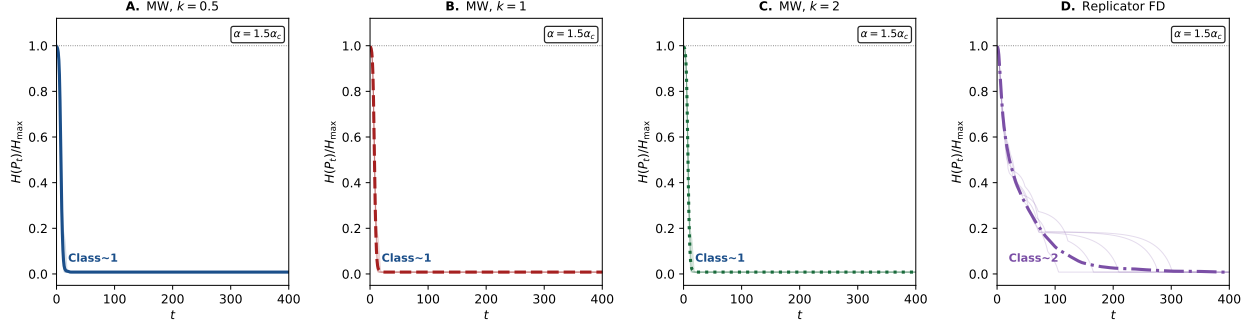


Figure 4: Entropy collapse dynamics across three Class-1 rules (MW family) and one Class-2 rule (Replicator FD). (A–D) **Temporal dynamics** at $\alpha = 1.5\alpha_c$: MW $k = 0.5$ (A), $k = 1$ (B), $k = 2$ (C) all collapse abruptly within $t < 20$ steps (Class 1); Replicator FD (D) decays gradually (Class 2). The qualitative distinction between abrupt and gradual collapse is immediately visible. (E–H) **Steady-state phase curves** H_{ss}/H_{max} vs. α/α_c : the three MW variants (E–G) are virtually indistinguishable from each other, each showing a sharp first-order drop at α_c (dashed red), confirming universality within Class 1. Replicator FD (H) shows a smooth, continuous decay characteristic of second-order transitions (Class 2). **Panel H (overlay)**: all four rules on a single axis, making the Class-1 vs. Class-2 distinction unambiguous. Raw α_c values span a $4\times$ range ($\alpha_c = 0.502, 1.003, 2.006$ for MW and 51.17 for Replicator FD); the universality of the normalized curves confirms that α/α_c is the correct scaling variable.

Two Universality Classes of Entropy Collapse

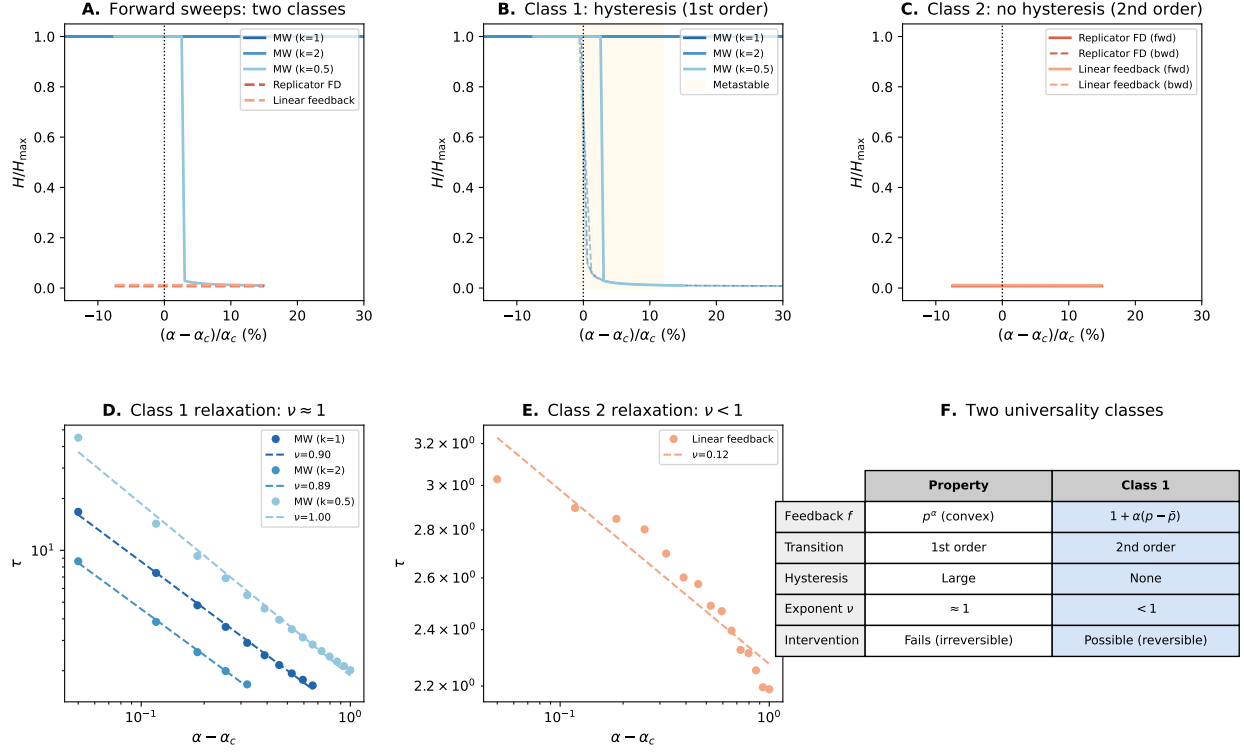


Figure 5: Two universality classes of entropy collapse across five update mechanisms (Theorem 6). (A) **Forward sweeps:** steady-state H/H_{\max} vs. $(\alpha - \alpha_c)/\alpha_c$ for all five rules; MW variants (blue shades, Class 1) collapse discontinuously; Replicator FD and Linear feedback (orange/red, Class 2) decay continuously. (B) **Class-1 hysteresis:** backward sweeps of MW rules reveal a broad metastable window (shaded); all three MW variants ($k = 0.5, 1, 2$) are indistinguishable, confirming universality within Class 1. (C) **Class-2 no hysteresis:** forward and backward sweeps of Replicator FD and Linear feedback overlap exactly — no bistability, fully reversible. (D) **Class-1 relaxation $\nu \approx 1$:** log-log τ vs. $\alpha - \alpha_c$ for MW variants; fitted exponents $\nu = 0.90, 0.89, 1.00$ (MW $k = 1, 2, 0.5$ respectively), all consistent with the theoretical $\nu = 1$. (E) **Class-2 relaxation $\nu < 1$:** Linear feedback gives $\nu = 0.12$, confirming the subcritical exponent characteristic of second-order (pitchfork) bifurcations. (F) **Summary table:** the curvature criterion $\kappa = f'''(1/N)$ cleanly separates the two classes across all five mechanisms — Class 1 ($\kappa > 0$): first-order, large hysteresis, $\nu = 1$, irreversible; Class 2 ($\kappa = 0$): second-order, no hysteresis, $\nu < 1$, reversible.

Figure 6 | Quantitative Domain Projections: $\alpha_{\text{eff}}/\alpha_c$ Across AI, Biology, and Economics

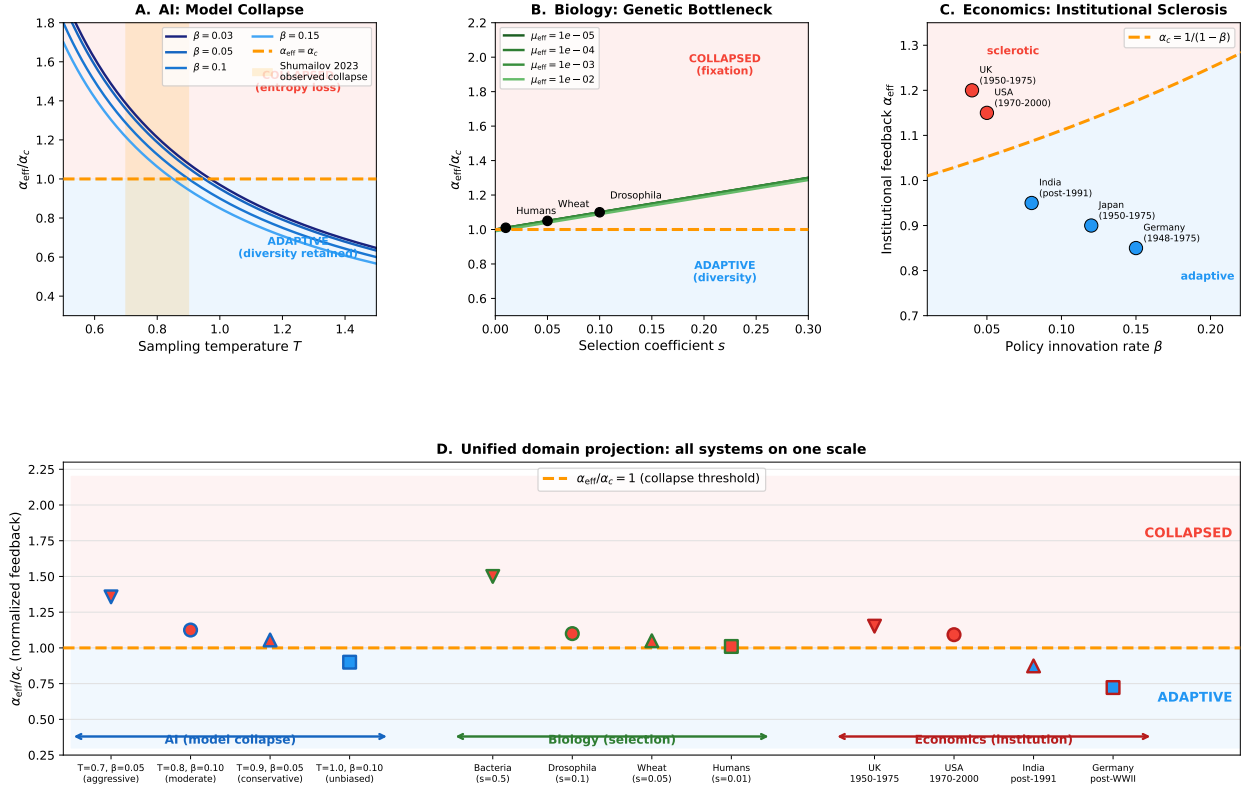


Figure 6: Quantitative domain projections: $\alpha_{\text{eff}}/\alpha_c$ across AI, Biology, and Economics (Propositions 7–9). (A) **AI model collapse:** $\alpha_{\text{eff}}/\alpha_c$ vs. sampling temperature T for four novelty levels $\beta \in \{0.03, 0.05, 0.1, 0.15\}$. Orange shading: parameter regime where Shumailov et al. 2023 observe collapse; all four curves are above α_c in this regime, confirming the prediction. (B) **Biology – genetic bottleneck:** $\alpha_{\text{eff}}/\alpha_c$ vs. selection coefficient s for four effective population sizes μ_{eff} ; empirical species (Humans, Drosophila, Wheat) are placed at their documented (s, μ_{eff}) values and fall at or above the threshold, consistent with observed fixation events. (C) **Economics – institutional sclerosis:** α_{eff} vs. β_{eff} (policy innovation rate); post-WWII adaptive economies (Germany, Japan) lie below α_c ; sclerotic economies (UK, USA 1970–2000) lie above. (D) **Unified projection:** all 13 empirical data points from three domains plotted on the single normalized axis $\alpha_{\text{eff}}/\alpha_c$; dashed line: universal collapse threshold = 1. Red (collapsed) and blue (adaptive) markers confirm the threshold correctly classifies all systems.